

## Vacancy-hole and vacancy-tube migration in multiwall carbon nanotubes

J. Y. Huang,<sup>1,\*</sup> F. Ding,<sup>2</sup> and B. I. Yakobson<sup>2</sup>

<sup>1</sup>*Center for Integrated Nanotechnologies (CINT), Sandia National Laboratories, Albuquerque, New Mexico 87185, USA*

<sup>2</sup>*Department of Mechanical Engineering and Materials Science, and Department of Chemistry, Rice University, Houston, Texas 77005, USA*

(Received 17 September 2008; published 29 October 2008)

Evidence is presented that vacancy-hole or vacancy-tube (similar to vacancy loops in crystalline materials) migration constitutes an important self-diffusion mechanism in multiwall carbon nanotubes (MWCNTs) when they were irradiated by an electron beam at about 2000 °C. Isolated vacancies agglomerated to form vacancy holes/tubes with lengths from 3 to 16 nm and widths from 1 to 4 basal planes in the intermediate layers of the MWCNTs. The formation of vacancy holes/tubes is attributed to the high mobility of vacancies at high temperatures and the confinement of the intermediate layers posed by the top and bottom layers. The vacancy holes/tubes were mobile and could migrate along the axial, radial, or circumferential directions of the nanotubes. Driven by the temperature gradient and the thermal fluctuation, the migration velocity of the holes varies from a few to 80 nm/s. The results demonstrate that a carbon nanotube is a perfect system for studying vacancy properties in a quasi-one-dimensional system.

DOI: 10.1103/PhysRevB.78.155436

PACS number(s): 61.72.Lk, 62.20.F-, 62.25.-g, 68.37.Lp

### I. INTRODUCTION

Point defects such as vacancies affect the physical and chemical properties of carbon nanotubes (CNTs) significantly.<sup>1–17</sup> For example, a single vacancy in a single wall carbon nanotube (SWCNT) can reduce its mechanical strength<sup>1–3</sup> and its electrical conductivity dramatically.<sup>4–6</sup> Vacancies also control the operation of nanotube-based chemical sensors and affect the functionalization of CNTs.<sup>7</sup> Therefore understanding the formation and migration of vacancies in CNTs is indispensable for tailoring their electrical, mechanical, and chemical properties and controlling irradiation-induced transformations in these systems.

The discovery of vacancy-mediated diffusion in metals and alloys, the Kirkendall effect,<sup>18–21</sup> revolutionized the physical metallurgy field. As a consequence of the Kirkendall effect in bulk crystals—and here in multiwall CNTs (MWCNTs)—the irradiation of carbon (for example in a nuclear reactor or under electron beam) creates vacancies and interstitials,<sup>22–26</sup> which are mobile, and can mutually annihilate or migrate to the surface or another sink such as a void or a dislocation. In particular, if an excess of one defect occurs, it leads to its condensation dislocation loops, or voids, or vacancy disks. Further, these mesoscopic and easily observable aggregates can migrate as a result of atom or vacancy diffusion. Recently, high-resolution transmission electron microscopy (HRTEM) evidence of diffusion and migration of large vacancy clusters and nanometer-sized dislocation loops attracted keen interest.<sup>15–17,27,28</sup> Here we present the formation and migration of large vacancy aggregates in CNTs, which are heated to very high temperatures in high vacuum. Different from that in bulk materials, the interstitials created by electron irradiation or thermal activation are easily sublimated to vacuum and, as a consequence, the increasing vacancy concentration must result in large fold vacancy formations, e.g., vacancy holes and even vacancy tubes.

### II. EXPERIMENTS

Our experiments were conducted inside a HRTEM attached with a Nanofactory transmission electron

microscopy-scanning tunneling microscopy (TEM-STM) platform. The MWCNTs were synthesized by an arc discharge method. Individual carbon fibers from the arc-discharged soot were glued to a Au rod with a diameter of 250  $\mu\text{m}$ . Individual MWCNTs were connected to the STM probe and heated to high temperatures by applying a high bias voltage.

### III. RESULTS AND DISCUSSION

Figure 1 shows the vacancy-hole dynamics in a MWCNT. Initially a small hole was opened on the left walls (denoted by a set of dotted lines near the hollow of the MWCNT), which then expanded its size along the edge of the same walls [Figs. 1(b) and 1(c)] until a vacancy tube was formed [Figs. 1(d)–1(f)]. Concurrently, a second hole was formed (marked by a set of dotted lines near the surface of the MWCNT), and it grew in a similar fashion as the first one [Figs. 1(c)–1(f)]. The two holes are just four walls apart [Fig. 1(b)], yet they did not merge with each other, implying a high vacancy migration barrier along the radial directions. In contrast, vacancies were easily migrated in the same basal planes. The hole near the nanotube hollow moved downward at a velocity of 1.5 nm/min and grew toward the two ends of the MWCNT to a length of 7 nm [Figs. 1(d) and 1(e)]. The hole near the nanotube surface grew toward the two ends of the MWCNT to form a long vacancy tube with a length of about 10 nm [Figs. 1(d) and 1(e)]. Figures 1(g)–1(l) are structural models showing how the removal of carbon atoms can generate vacancy holes/tubes in a MWCNT.

Figure 2 shows the formation and migration of two vacancy holes in a MWCNT. Both holes were nucleated from the right walls, and then extended toward the left walls along the same basal planes. The termination edges of the holes are seen clearly (see the dotted lines). The upper loop appeared to have extended through the entire circumference along the same walls [Fig. 2(c)], thus forming a vacancy tube having the same axis as the nanotube. The lower hole did not extend through the whole circumference, but it migrated from the

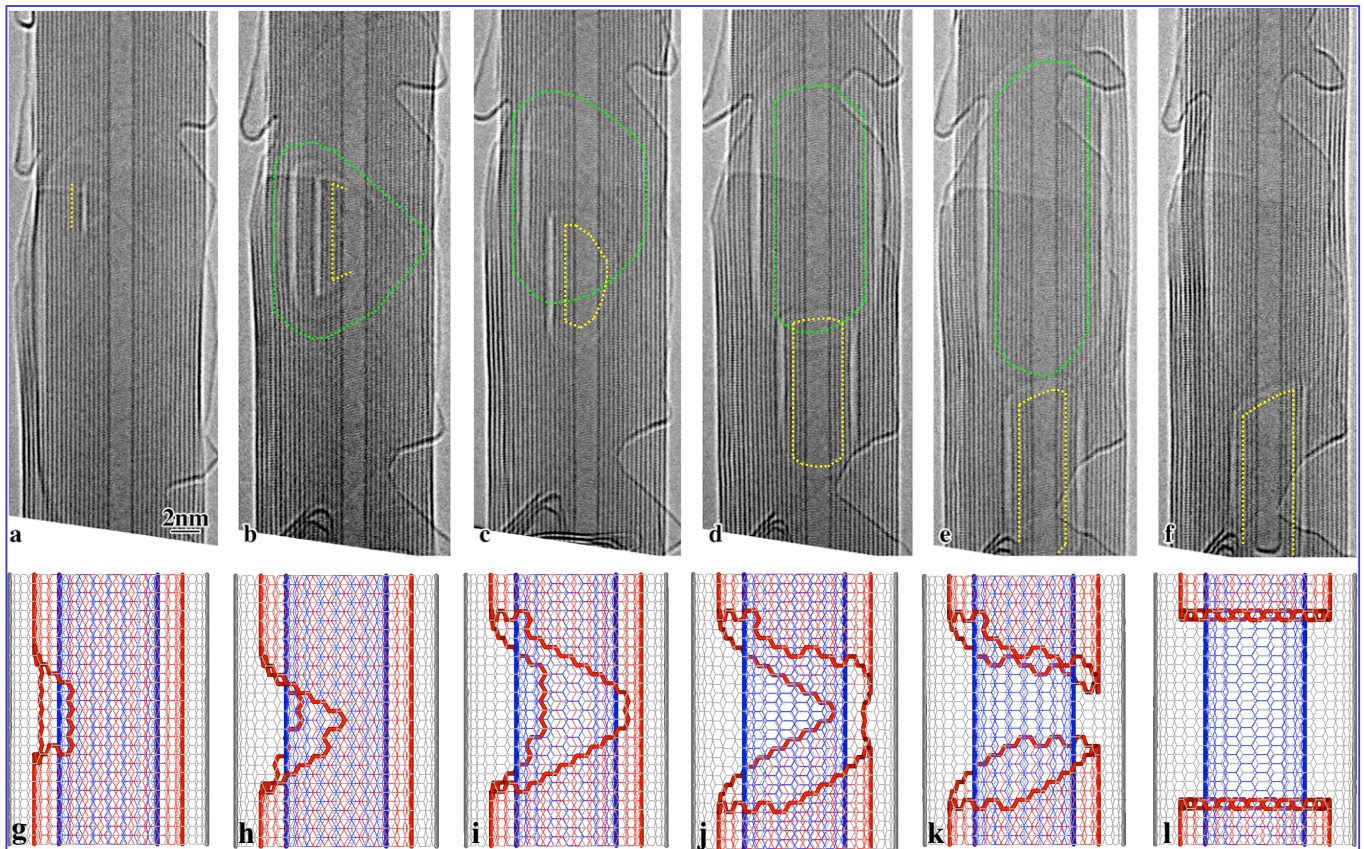


FIG. 1. (Color online) (a)–(f) Formation and migration of two vacancy holes/tubes (outlined by two sets of dotted lines near the hollow and surface of the MWCNT, respectively) in a MWCNT irradiated by electron beam at about 2000 °C. Note both the shape and position changes of the holes. In (c) the upper hole extended through the entire circumference, forming a vacancy tube. The length and width of the upper hole are 6 nm and three-wall thickness, respectively, and those of the lower hole are 4 nm and three-wall thickness, respectively. (g)–(l) Schematic drawing showing how a vacancy hole/tube is formed due to removal of C atoms.

right wall to the left wall. In the mean time it also crossed one wall inward along the radial direction. A schematic drawing showing how the lower vacancy hole [Figs. 2(a)–2(c)] migrated along the circumference is shown in Figs. 2(d)–2(f). Figures 2(g)–2(j) show the migration of a hole (or glide of a dislocation loop) from an outer layer to an inner layer. Figure 2(i) shows the side and bottom views of the intermediate dislocation loop. Two edge dislocations in the outer layer [shown by a light gray line on top of Fig. 2(i)] and the inner layer [shown by a gray line on the bottom of Fig. 2(i)] are connected together by two screw dislocations and form a complete dislocation loop. The two screw dislocations glide together along the two bent arrows and cancel each other. Thus the dislocation loop (or the vacancy hole) migrates to the inner wall completely [Fig. 2(j)].

Figure 3 shows the formation of a giant hole on the surface wall of a MWCNT (movie M1) due to the sublimation of carbon atoms. Initially a hole was opened on the surface wall [Fig. 3(b)], and it then expanded continuously toward the two ends of the MWCNT until the surface wall was entirely disconnected [Figs. 3(c)–3(e)]. During the expansion process, the edges of the holes changed from a plane inclined to the tube axis [Figs. 3(b)–3(d)] to one being perpendicular to the tube axis [Fig. 3(e)]. Note that once the surface wall was broken, the two broken segments receded continuously

toward the two ends of the MWCNT in a similar speed, meaning that the atom removal process was not notably affected by the polarity of the electrode, and electromigration was not playing a dominant role in the hole migration process.

Figure 4 (movie M2) shows vacancy dynamics in another MWCNT. The vacancy (outlined by dotted lines) remained at the same basal planes while it migrated at a velocity of 5 nm/min downward. During the migration process, the hole grew from the right wall toward the left wall following the same basal planes. The hole on the right wall remained almost the same size during the migration process. Apparently mass transport has occurred during the vacancy migration process, since atoms were added to the upper edge and removed from the lower edge of the vacancy hole.

The migration velocity of small vacancy holes was generally faster than that of the large holes. For small holes, a velocity of up to 80 nm/min was observed (movie M3). For large holes, the velocity was usually less than 10 nm/min. Very frequently, the holes moved up and down repeatedly in a manner similar to a one-dimensional Brownian motion, but overall the holes migrated downward the tube axis (Figs. 1 and 4). Note that there was no current flowing in the nanotubes shown in Figs. 1 and 4, since it was attached to a bigger nanotube (where the current flowed) on one end and



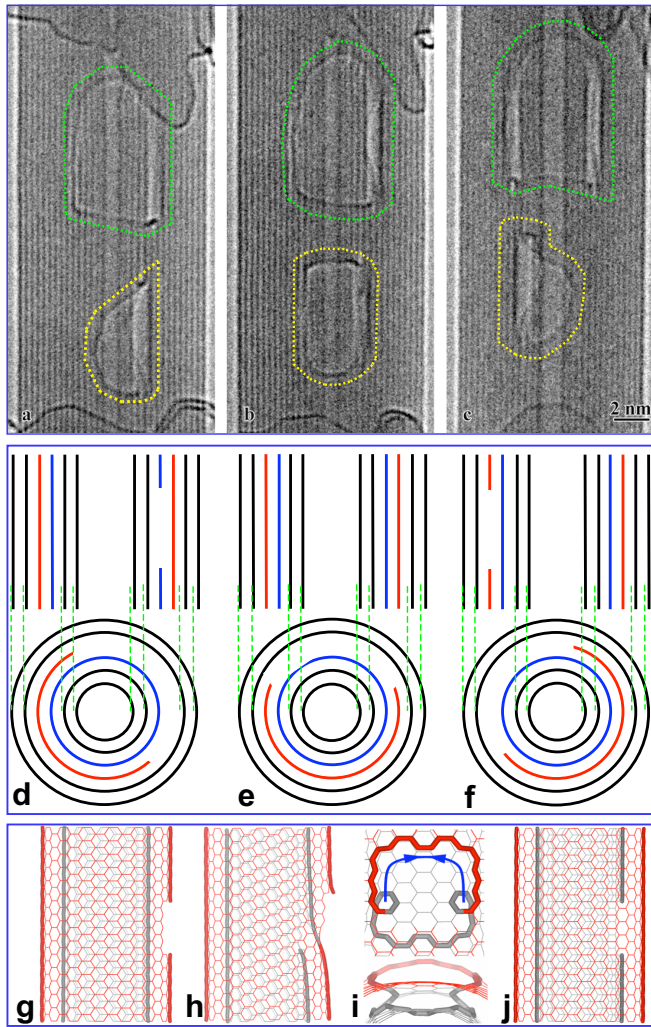


FIG. 2. (Color online) (a)–(c) Formation and migration of two vacancy loops (outlined by two sets of dotted lines on top and bottom of the figure, respectively) in a MWCNT irradiated by an electron beam at about 2000 °C. Note both the shape and position changes of the loops. In (c) the upper loop extended through the entire circumference, forming a vacancy tube with the same axis as the nanotube. The nanotube was joule heated at 2.26 V and 111  $\mu$ A. (d)–(e) and (g)–(j) are schematic drawings showing how the lower vacancy hole in Figs. 2(a)–2(c) migrated along the circumferential and the radial directions of the tube, respectively.

suspended on the other end [Fig. S1 (Ref. 30)]. So the vacancy migration was not driven by electromigration. The driving force for the hole migration might be the temperature gradient and/or thermal fluctuation in the nanotubes. As shown in Fig. S1 (Ref. 30), one end of the MWCNT (the down side) is attached to a bigger tube which was joule heated by current flow. So the temperature of the upper side should be lower than that of the down side or the temperature gradient is downward. Our observation indicates that overall a vacancy flows toward the direction of the temperature gradient (or from cold regions toward hot regions) as theoretically predicted.<sup>31</sup> The observation is consistent with a recent report on a cargo motion along a MWCNT driven by a temperature gradient.<sup>32</sup>

Based on the above observations, we propose the following vacancy formation and migration mechanism. At first, isolated vacancies were generated in the nanotubes due to evaporation (by heat) or knock out (by electron beam) of carbon atoms from the tube wall.<sup>2</sup> These vacancies aggregated to form vacancy holes to lower the energy of the system, as shown in a molecular-dynamics (MD) simulation [Figs. 5(a)–5(f)]. The hole then moved upward or downward and in the mean time expanded its size. For the hole to move upward or downward, a mass transfer is required, or in other words, the vacancy-hole migration is driven by atom transport; e.g., atoms at the upper edge of the hole moving downward lead the vacancy hole to move upward [e.g., Figs. 5(g) and 5(h)]. There are two possible atom transport mechanisms in the hole, i.e., C atoms are evaporated from one side of the hole and then deposited on the opposite side [Figs. 5(g) and 5(h)] or C atoms diffuse along the hole edges and migrate from one side to the other side [Figs. 5(d)–5(f)]. The latter mechanism has a much lower diffusion barrier [only  $\sim 1.62$ – $2.14$  eV, as shown in Figs. 5(i) and 5(j)] than the former. Therefore C atoms migrating along the open edges of the vacancy hole dominate the hole migration process [Figs. 5(d)–5(f), arrowheads, movie M4].

Vacancy holes/tubes in a SWCNT were not observed under similar experimental conditions as that in MWCNTs. In fact, atomistic analysis indicates that large holes in a SWCNT are energetically unfavorable.<sup>10</sup> Indeed, a SWCNT can heal the hole by shrinking its diameter when it is irradiated.<sup>35,36</sup> Once vacancies are formed in a SWCNT, it immediately self-repairs by the formation of 5|7 defects, which then serve as scavengers for further defects, thus pre-

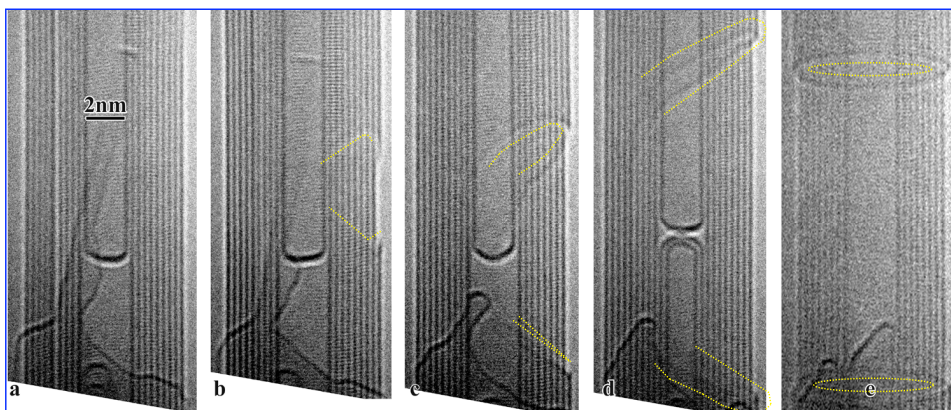


FIG. 3. (Color online) Growth and migration of a vacancy hole on the surface wall of a MWCNT. The dotted lines outline the shape and size of the holes.

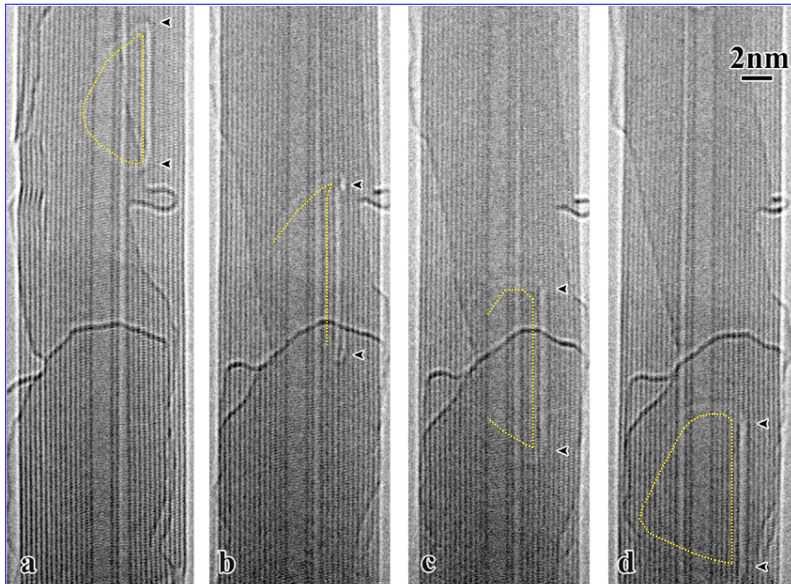


FIG. 4. (Color online) Migration of a vacancy hole (outlined by dotted lines and arrowheads) with a velocity of 5 nm/min downward the tube axis when the nanotube was irradiated at 2000 °C (Ref. 29) (movie M1). While the hole moved downward, it also expanded along the circumferential direction. The bias voltage applied to the nanotube was 2.55 V. The length and width of the vacancy hole are 10 nm and two-wall thickness, respectively. Note that the innermost two walls were detached from the rest of the walls, which was caused by the diameter shrinkage of the nanotube induced by vacancy generation and reconstruction.

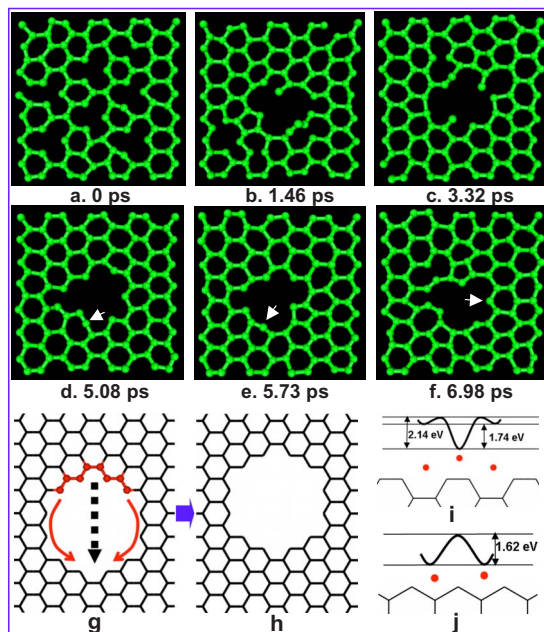


FIG. 5. (Color online) MD simulation of vacancy aggregation [(a)→(c)] and interstitial diffusion along the edge of a vacancy hole [(d)→(f)]. The migration barriers were calculated by the semi-empirical PM3 method and the MD simulation was done with a density-functional-based tight-binding (DFTB) method (Refs. 33 and 34). In the MD simulation, a graphene described by a periodic boundary condition was used to model a wall in the middle of a MWCNT, which cannot shrink as a SWCNT due to the confinement of the inner walls. The simulation starts with six single vacancies. At 3500 K, the six vacancies evolve into a vacancy hole [(a)→(b)→(c)] by vacancy aggregation. The arrows mark an atom migrating along an atom edge of a hole [(d)→(e)→(f)]. The MD time step is 0.5 fs. (g),(h) C atoms are evaporated from the upper edge of the hole and deposited at the lower edge, causing the hole to move upward. (i),(j) Potential barrier for a C atom to migrate along the armchair and zigzag edges of a graphene.

venting the formation of large holes as observed in a MWCNT.

For those walls that are sandwiched between the top and bottom layers in a MWCNT, the shrinking mechanism operating in a SWCNT does not work because of the confinement of the top and bottom layers. As a result, the vacancies in a sandwiched layer can neither escape nor relax, but agglomerate to form vacancy holes. However, for the innermost and the outermost layers in a MWCNT, the lack of confinement led to very different scenarios, namely, vacancies are able to relax in the innermost layer in a way similar to that in a SWCNT. As a result, the innermost layer was able to shrink its diameter, which was indeed observed in our experiments (e.g., Fig. 4, in this case, the innermost two layers were shrinking). In fact, because of the shrinkage of the innermost one or two layers, they were detached from the other outer layers. For the outermost layer, C atoms were sublimated to the vacuum quickly, leading to the rapid expansion of the holes in the surface layer, which was frequently observed in our experiments (e.g., Fig. 3).

#### IV. CONCLUSIONS

Vacancy holes and vacancy tubes were formed in MWCNTs when they were irradiated by an electron beam at about 2000 °C. The vacancy holes/tubes were mobile and could migrate along the axial, radial, or circumferential directions of the nanotubes. The formation of vacancy holes/tubes is attributed to the high mobility of vacancies at high temperatures, and the confinement of the intermediate layers posed by the top and bottom layers. Driven by the temperature gradient and the thermal fluctuation, the migration velocity of the holes varies from a few to 80 nm/s. The formation of vacancy holes/tubes in MWCNTs may offer new opportunities to engineer the structure and properties of MWCNTs for specific device applications, and the functionalization of MWCNTs. Our findings also demonstrate that a CNT is a perfect system for studying vacancy behavior in a quasi-one-dimensional system.



## ACKNOWLEDGMENTS

This work was supported in part by the Center for Integrated Nanotechnologies, a U.S. Department of Energy (DOE), Office of Basic Energy Sciences (BES) user facility, and in part by the DOE Office of BES, Division of Materials

Science and Engineering. Sandia is a multiprogram laboratory operated by Sandia Corporation, a Lockheed Martin Co., for the U.S. Department of Energy's National Nuclear Security Administration under Contract No. DE-AC04-94AL85000. J.Y.H. would like to thank Ju Li from the University of Pennsylvania for his comments and suggestions.

\*Corresponding author; [jhuang@sandia.gov](mailto:jhuang@sandia.gov)

- <sup>1</sup>T. Dumitrica, M. Hua, and B. I. Yakobson, Proc. Natl. Acad. Sci. U.S.A. **103**, 6105 (2006).
- <sup>2</sup>F. Ding, K. Jiao, Y. Lin, and B. I. Yakobson, Nano Lett. **7**, 681 (2007).
- <sup>3</sup>F. Ding, K. Jiao, M. Q. Wu, and B. I. Yakobson, Phys. Rev. Lett. **98**, 075503 (2007).
- <sup>4</sup>C. Gomez-Navarro, P. J. De Pablo, J. Gomez-Herrero, B. Biel, F. J. Garcia-Vidal, A. Rubio, and F. Flores, Nature Mater. **4**, 534 (2005).
- <sup>5</sup>H. J. Choi, J. Ihm, S. G. Louie, and M. L. Cohen, Phys. Rev. Lett. **84**, 2917 (2000).
- <sup>6</sup>A. Hansson, M. Paulsson, and S. Stafstrom, Phys. Rev. B **62**, 7639 (2000).
- <sup>7</sup>J. A. Robinson, E. S. Snow, S. C. Badescu, T. L. Reinecke, and F. K. Perkins, Nano Lett. **6**, 1747 (2006).
- <sup>8</sup>A. V. Krasheninnikov, K. Nordlund, M. Sirvio, E. Salonen, and J. Keinonen, Phys. Rev. B **63**, 245405 (2001).
- <sup>9</sup>A. V. Krasheninnikov, P. O. Lehtinen, A. S. Foster, and R. M. Nieminen, Chem. Phys. Lett. **418**, 132 (2006).
- <sup>10</sup>J. Kotakoski, A. V. Krasheninnikov, and K. Nordlund, Phys. Rev. B **74**, 245420 (2006).
- <sup>11</sup>M. Terrones, F. Banhart, N. Grobert, J. C. Charlier, H. Terrones, and P. M. Ajayan, Phys. Rev. Lett. **89**, 075505 (2002).
- <sup>12</sup>A. J. Lu and B. C. Pan, Phys. Rev. Lett. **92**, 105504 (2004).
- <sup>13</sup>S. Zhang, S. L. Meilke, R. Khare, D. Troya, R. S. Ruoff, G. C. Schatz, and T. Belytschko, Phys. Rev. B **71**, 115403 (2005).
- <sup>14</sup>F. Banhart, Rep. Prog. Phys. **62**, 1181 (1999).
- <sup>15</sup>A. Hashimoto, K. Suenaga, A. Gloter, K. Urita, and S. Iijima, Nature (London) **430**, 870 (2004).
- <sup>16</sup>K. Urita, K. Suenaga, T. Sugai, H. Shinohara, and S. Iijima, Phys. Rev. Lett. **94**, 155502 (2005).
- <sup>17</sup>C. Jin, K. Suenaga, and S. Iijima, Nano Lett. **8**, 1127 (2008).
- <sup>18</sup>E. Kirkendall, JOM **51**, 54 (1999).
- <sup>19</sup>E. Kirkendall, L. Thomassen, and C. Uethegrove, Trans. Am. Inst. Min., Metall. Pet. Eng. **133**, 186 (1939).
- <sup>20</sup>E. O. Kirkendall, Trans. Am. Inst. Min., Metall. Pet. Eng. **147**, 104 (1942).
- <sup>21</sup>A. D. Smigelskas and E. O. Kirkendall, Trans. Am. Inst. Min., Metall. Pet. Eng. **171**, 130 (1947).
- <sup>22</sup>C. P. Ewels, M. I. Heggie, and P. R. Briddon, Chem. Phys. Lett. **351**, 178 (2002).
- <sup>23</sup>C. P. Ewels, R. H. Telling, A. A. El-Barbary, M. I. Heggie, and P. R. Briddon, Phys. Rev. Lett. **91**, 025505 (2003).
- <sup>24</sup>B. T. Kelly, *Physics of Graphite* (Applied Science, London, 1981).
- <sup>25</sup>R. H. Telling, C. P. Ewels, A. A. El-Barbary, and M. I. Heggie, Nature Mater. **2**, 333 (2003).
- <sup>26</sup>K. Nordlund, J. Keinonen, and T. Mattila, Phys. Rev. Lett. **77**, 699 (1996).
- <sup>27</sup>K. Arakawa, K. Ono, M. Isshiki, K. Mimura, M. Uchikoshi, and H. Mori, Science **318**, 956 (2007).
- <sup>28</sup>Y. Matsukawa and S. J. Zinkle, Science **318**, 959 (2007).
- <sup>29</sup>J. Y. Huang, Nano Lett. **7**, 2335 (2007).
- <sup>30</sup>See EPAPS Document No. E-PRBMDO-78-059839 for supporting movies showing vacancy migration in a MWCNT, and a supporting figure showing that there is no current flow in the MWCNT. For more information on EPAPS, see <http://www.aip.org/pubservs/epaps.html>.
- <sup>31</sup>W. Shockley, Phys. Rev. **91**, 1563 (1953).
- <sup>32</sup>A. Barreiro, R. Rurali, E. R. Hernandez, J. Moser, T. Pichler, L. Forro, and A. Bachtold, Science **320**, 775 (2008).
- <sup>33</sup>D. Porezag, T. Frauenheim, T. Kohler, G. Seifert, and R. Kaschner, Phys. Rev. B **51**, 12947 (1995).
- <sup>34</sup>C. M. Goringe, D. R. Bowler, and E. Hernandez, Rep. Prog. Phys. **60**, 1447 (1997).
- <sup>35</sup>J. Y. Huang, S. Chen, Z. Q. Wang, K. Kempa, Y. M. Wang, S. H. Jo, G. Chen, M. S. Dresselhaus, and Z. F. Ren, Nature (London) **439**, 281 (2006).
- <sup>36</sup>J. Y. Huang, S. Chen, Z. F. Ren, Z. Wang, K. Kempa, M. J. Naughton, G. Chen, and M. S. Dresselhaus, Phys. Rev. Lett. **98**, 185501 (2007).